Quasi-elastic Electron-Neutron Scattering in ^{4}He

A. Misiejuk[1], Z. Papandreou[2], E. Voutier[3], Th.S. Bauer[4], H.P. Blok[5], D.J. Boersma[1], H.W. den Bok[1], E.E.W. Bruins[1], F. Farzanpay[2], K. Grüner[3], W.H.A. Hesselink[5], G.M. Huber[2], E. Jans[4], N. Kalantar-Nayestanaki[6], W.-J. Kasdorp[4], J. Konijn[4], J.-M. Laget[7], L. Lapikás[4], G.J. Lolos[2], G.J.G. Onderwater[5], A. Pellegrino[5], R. Schroevers[4], C.M. Spaltro[4], R. Starink[5], G. van der Steenhoven[4], J.J.M. Steiger[4], J.L. Visschers[4], H.W. Willering[1], D.M. Yeomans[1]

[1] *Universiteit Utrecht/NIKHEF, P.O.Box 80000, 3508 TA Utrecht, The Netherlands*
[2] *Department of Physics, University of Regina, Regina, Saskatchewan, S4S 0A2, Canada*
[3] *Institut des Sciences Nucléaires, IN2P3-CNRS/UJF, 53 Avenue des Martyrs, 38026 Grenoble, France*
[4] *NIKHEF, P.O.Box 41822, 1009 DB Amsterdam, The Netherlands*
[5] *Department of Physics and Astronomy, Free University, 1081 HV Amsterdam, The Netherlands*
[6] *KVI, Zernikelaan 25, 9747 AA Groningen, The Netherlands*
[7] *CEA-Saclay, Service de Physique Nucléaire, 91191 Gif-sur-Yvette CEDEX, France*

(January 31, 2002)

The differential cross section for quasi-elastic neutron knockout in the reaction ^{4}He(e,e′n)^{3}He, at a momentum transfer of 300 MeV/c and in the missing momentum range of 25-70 MeV/c, has been measured for the first time with a statistical accuracy of 11 %. The comparison of the data with theoretical calculations shows that, in this kinematical regime, the cross section is dominated by final state interaction effects, and particularly by the p-n charge exchange process.

PACS numbers: 13.40.Gp, 14.20.Dh, 25.30.Fj

During the past decades, (e,e′N) electron-nucleon quasi-elastic scattering (QES) has provided us with a wealth of data allowing us to study, *e.g.*, nuclear structure, the role of subnucleonic degrees of freedom in reaction mechanisms and the electromagnetic form factors of nucleons.

Nearly all QES data on nuclei heavier than ^{3}He have been obtained from the proton-knockout reaction in two-spectrometer coincidence experiments [1]. It is desirable to avail of QES data for the neutron knock-out reaction, in particular for the study of electromagnetic form factors and neutron bound-state wave functions. Before such issues can be addressed, the mechanism of the (e,e′n) reaction needs to be understood.

Within the framework of the Plane Wave Impulse Approximation (PWIA), the cross section for this knockout reaction can be factorized into the product of the elementary e-N cross section, a spectral function, and kinematical factors. However, this first order picture has been proven incomplete (*e.g.* Ref. [2,3]): additional mechanisms must be considered, such as Meson Exchange Currents (MEC), rescattering or Final State Interactions (FSI), as well as nuclear medium modifications of basic particle properties.

Unlike proton knockout, the (e,e′n) channel remains largely unexplored, and no data are available for nuclei with mass $A \geq 4$. The reason for this is that for momentum transfers of a few hundred MeV/c and small scattering angles, the corresponding coupling of the virtual photon to the neutron is 5 to 10 times weaker than the coupling to the proton. This, compounded with a typical detection efficiency for neutrons of about 10 %, makes this channel very difficult to access.

The mechanism of the (e,e′n) reaction was first studied in the pioneering work of Daman [4], in which the recoil technique was used to measure the reaction ^{4}He(e,e′ ^{3}He)n. These data confirm that quasi-elastic proton and neutron knockout differ substantially. PWIA, which usually overestimates experimental cross sections in the case of (e,e′p) reactions, falls short by about half an order of magnitude for the case of the ^{4}He(e,e′ ^{3}He)n reaction. The author argues that p-n rescattering is responsible for providing the additional strength in the neutron knockout channel. Charge-exchange potentially affects every nucleon-knockout reaction, and thus must be fully understood.

In view of the absence of reliable data on e-n QES, the first goal is to establish a precise value for the cross section under quasi-elastic kinematics. This is the motivation behind the work presented in this Letter. The ^{4}He target was chosen because of its well-understood structure allowing for reliable theoretical calculations. In particular, protons and neutrons occupy similar states. In addition, the high nuclear density is expected to enhance charge-exchange effects. Finally, ^{4}He is an extensively studied nucleus for which, in addition to inclusive electron scattering, extensive quasi-elastic proton knockout data are available [2,3,5–7].

The ^{4}He(e,e′n)^{3}He experiment was performed at the accelerator complex MEA-AmPS of NIKHEF, Amsterdam, using an electron beam of 586 MeV with an average intensity of 1 μA and a 50 % duty cycle. Incident electrons impinged radially on a ^{4}He gas target (at 15 K and 1 MPa) contained in a cylindrical vessel of 5 cm diameter with wall thickness of 0.2 mm Al. The relative target thickness was monitored throughout the experiment by counting single events from the (e,e′) reaction

in the QDD magnetic spectrometer [8].

The QDQ magnetic spectrometer [9] was used to detect electrons in coincidence with neutrons which were detected in a time-of-flight (ToF) plastic scintillator detector array. The QDQ – whose acceptance was collimated to subtend a solid angle $\Delta\Omega$ = 9.6 msr and a momentum bite of 10 % – was placed at 30.79°. This resulted in a central momentum transfer q=300 MeV/c and an energy transfer ω=84 MeV.

The neutron ToF detector had been used previously for precision measurements of the magnetic form factor of the neutron [10,11]. The detector consisted of five NE102A plastic scintillators, having frontal dimensions of 25×25 cm^2, each read out by a single photomultiplier tube (PMT). The first three detectors (ΔE_i, i=1,2,3) were 1 mm thick and served to distinguish charged from neutral particles. These were followed by two 50-mm-thick detectors (E_1 and E_2). All five scintillators were tilted by 30 ° with respect to the vertical plane in order to optimize the timing resolution. Between the two thick scintillators, a 1-cm-thick iron plate was placed so that no protons, in coincidence with the electrons detected in the spectrometer, could reach E_2. In this way, the signal in E_2 is due exclusively to neutrons, and was used to establish the losses of neutrons in E_1 due to pile-up of noise in the ΔE_i detectors. The neutron detector was positioned along the momentum transfer vector, at $-58.9°$ with respect to the beam, and at a distance of 7.8 m from the target center, thus subtending a solid angle of 1.1 msr. The assembly was surrounded by a shield consisting of 5 cm of lead and 25 cm of concrete, except at the front. There, the detector was shielded by a 1-mm-thick Pb plate which blocked low-energy background but was thin enough to allow the detection in E_1 of protons from the reaction ^{4}He(e,e′p)^{3}He. These events were used to calibrate the light response of the PMTs. In addition, a lead collimator of dimensions 10×1 cm^2 and thickness of 5 cm was placed in front of the 1 mm Pb sheet. This resulted in a limitation of the proton solid angle of the detector to 1/54 of the neutron one, and reduced data-acquisition dead time.

Neutrons and protons in the ToF detector were distinguished by their energy deposit in ΔE_i: the proton ADC signal was above a certain threshold value for all three ΔE_i, whereas the signal for neutrons corresponded to the pedestal value, slightly broadened due to pile-up. The permutational use of three veto detectors allowed the determination of the charged-particle-detection inefficiency and of the fraction of neutrons which scattered in the last veto counter. Neutrons were identified by requiring that the ADCs of two of the three ΔE_i counters were below threshold [10,11].

The track reconstruction of the detected electrons yielded a position resolution of 1 mm along the beam line that allowed the rejection of events originating from the target walls. Subsequently, cuts were applied to the time-of-flight of the electrons from the target to the spectrometer focal plane, and the timing walk was corrected. The set-up accepted a range of nucleon energies, which lead to a broadening of the raw coincidence signal. Based on the electron kinematics, the kinetic energy of quasi-elastic nucleons was determined and used to correct for this effect. Finally, in the case of protons, corrections for energy losses from the target to the detector were considered. All these resulted in a corrected ToF spectrum (Fig. 1a) with a signal-to-noise ratio of 2.6.

The missing-energy (E_m) spectrum is shown in Fig. 1b. It was obtained by integrating over the entire acceptance of the experiment after subtraction of the time-uncorrelated background. Neutrons from the ^{4}He(e,e′n)^{3}He channel are centered in a peak at 20.5 MeV. The contribution of the ^{4}He(e,e′n)pd and ^{4}He(e,e′n)ppn channels, which should show up at $E_m \geq$ 26 MeV, appears to be negligible under the kinematical conditions of this experiment.

The experimental cross section is deduced from the neutron yield after several corrections have been applied (see [12] for a more comprehensive discussion):

i) *Neutron detection efficiency.* The neutron-detection efficiency had been extensively studied and precisely measured in the past [10,11]. In the present experiment, the calibration of the ADC response was accomplished via the ^{4}He(e,e′p)^{3}H reaction. The detector response was simulated using the ENIGMA Monte Carlo code [13], with the uncertainty in these simulations proving to be negligible due to the small solid angle of the detector. The corrected neutron yield was found to be independent of the software ADC threshold, which establishes the validity of the efficiency correction. The relative uncertainty of this correction contains several contributions and was calculated to be 5.5 %.

ii) *Neutron losses.* Neutron losses resulting from interactions in the ΔE_i detectors were calculated by comparing the number of neutrons in the TDC peak of the E_2 spectrum, with and without the veto condition. Within the 10 % statistical uncertainty per bin (see below), the number of neutrons seen in the E_2 counter was the same for both cases, from which it was concluded that these losses were insignificant.

iii) *Proton misidentification.* A certain number of protons fall below the ΔE_i thresholds, and thus are misidentified as neutrons. However, due to the long flight-path, these protons show up in a separate missing energy peak when corrections for energy losses are not applied. The contribution of these events to the neutron yield was determined to be less than 1 %.

iv) *Neutron absorption.* Neutron absorption in the lead shield in front of the detector was simulated using ENIGMA [13] and GEANT [14] and found to be 5 %.

v) *Radiative corrections.* This correction results from the internal and external bremsstrahlung effects and was determined to be 18 %.

The experimental data in the acceptance range of 25-70 MeV/c were divided into three missing-momentum bins of equal width. Once all the aforementioned corrections were applied, the cross section for each bin was calculated by fitting the ground-state-transition peak in Fig. 1b. The result was not sensitive to the precise fitting parameters. The five-fold differential cross sections are given in Tab. 1, together with the statistical and the systematic uncertainties for each missing-momentum bin. The former has contributions from the experimental yield and the background substraction procedure, and was found to be uniformly 11 % for each p_m bin. An extensive study of the systematics [12] showed that they were dominated by the uncertainties in the neutron detection efficiency and the accuracy of the target thickness measurement, and were of the same order of magnitude as the statistical uncertainties.

Microscopic model calculations [15] of the ^{4}He(e,e′n) reaction have been performed using an extension of the diagrammatic approach [16]. The reaction amplitudes are expanded in terms of the relevant diagrams, and the elementary current operators are reduced from their relativistic form into a non-relativistic one, including all the terms up to (and including) order $1/m^3$ in the proton mass. For the initial ^{4}He and final ^{3}He states variational wave functions of the Urbana group [17] have been taken which are projected onto the various spin-isospin states of NN pairs, while half-off-shell NN scattering amplitudes are used in the final state. This model comprises one- (PWIA) and two-body (MEC, FSI) reaction mechanisms. Particularly, as depicted in Fig. 2, FSI take into account all the possible scatterings between the struck nucleon and a second nucleon, one of them being reabsorbed into the recoiling ^{3}He.

The comparison between the experimental cross section and theoretical calculations, averaged over the detector acceptance, is presented in Fig. 3. The full calculation reproduces the magnitude of the ^{4}He(e,e′n)^{3}He cross section. PWIA alone underestimates the experimental cross section significantly, in qualitative agreement with the findings of Daman [4]. The global effect of rescattering processes is to add strength to the (e,e′n) cross section. While elastic rescattering (Resc.) of the knocked-out neutron increases the discrepancy, the charge-exchange process (Exch.) of a proton hit by the electron (Fig. 2) provides the bulk of the cross section. In the momentum range covered by the experiment, the elastic neutron-rescattering amplitude is small, as compared to the quasi-elastic one, with which it interferes destructively. This is a direct consequence of unitarity, which shifts strength from the quasi-elastic peak to higher recoil momenta. On the contrary, the charge-exchange p-n rescattering FSI amplitude is driven by the Coulomb part of the proton electromagnetic current, which is strongly reduced in the quasi-elastic scattering of the electron off the neutron. In these kinematics, the MEC contribution suppresses the cross section by only 1 %.

Whereas the model is able to predict the magnitude of the ^{4}He(e,e′n)^{3}He cross section, it does not reproduce the slope of the momentum distribution. This may be due to the truncation of the multiple-scattering series to the first dominant term in the single scattering and calls to some extent for a complete treatment of the 4-body final state.

In summary, the reaction ^{4}He(e, e′n)^{3}He reaction was studied at a momentum transfer of 300 MeV/c for small missing-momentum and with a uncertainty of 11 %. Final-state interactions, mostly p - n charge-exchange, are the main causes for the large enhancement of the ^{4}He(e, e′n)^{3}He cross section over PWIA. The main effect of FSI is the net channeling of (e,e′p) strength into the (e,e′n) reaction from the two-step process (e,e′p)(p,n). The (e,e′n) reaction turns out to be more sensitive than the (e,e′p) channel to effects of reaction mechanisms. Clearly, whereas the charge exchange reaction moves strength between both QES channels, the effect is more pronounced in the electron-neutron reaction because of the larger cross section of the primary electron-proton channel.

This experiment is a blatant evidence of the different behaviour of (e,e′p) and (e,e′n) QES. A better understanding of the missing momentum variation calls for further theoretical and experimental investigations, especially in the context of the increasing number of proposals intending to use few body systems as neutron targets in electro-disintegration experiments.

The authors would like to thank A. van den Brink and the Utrecht mechanics team for their help during the experiment. This work was supported in part by the Stichting voor Fundamenteel Onderzoek der Materie (The Netherlands), the Natural Sciences and Engineering Research Council (Canada), NATO, and the Centre National de la Recherche Scientifique (France).

[1] J.J. Kelly, Adv. in Nucl. Phys. **23** (1996) 75.
[2] J.F.J. van den Brand *et al.*, Phys. Rev. Lett. **60** (1988) 2006; Phys. Rev. Lett. **66** (1991) 409.
[3] A. Magnon *et al.*, Phys. Lett. **B222** (1989) 352.
[4] M.A. Daman, Ph.D. Thesis, Universiteit van Amsterdam (1991);
H.P. Blok, Few Body Systems, suppl. 7 (1994) 120.
[5] J.-E. Ducret *et al.*, Nucl. Phys. **A556** (1993) 373.
[6] J.-M. Le Goff *et al.*, Phys. Rev. **C50** (1994) 2278.
[7] J.J. van Leeuwe *et al.*, Phys. Rev. Lett. **80** (1998) 2543.
[8] L. de Vries *et al.*, Nucl. Instr. Meth. Phys. Res. **A292** (1990) 629.

[9] C. de Vries *et al.*, Nucl. Instr. Meth. **223** (1984) 1.
[10] F.C.P. Joosse, Ph.D. Thesis, Universiteit Utrecht (1993); H. Anklin *et al.*, Phys. Lett. **B 336** (1994) 313.
[11] E.E.W. Bruins, Ph.D. Thesis, Universiteit Utrecht (1995); E.E.W. Bruins *et al.*, Phys. Rev. Lett. **75** (1995) 21.
[12] A. Misiejuk, Ph.D. Thesis, Universiteit Utrecht (1997).
[13] J.L. Visschers, in *MC93 International Conference on Monte Carlo Simulations in High Energy and Nuclear Physics*, Edts. P. Dragovitsch, S.L. Linn and M. Burbank (World Scientific Publishing Co., Singapore, 1994) 350.
[14] R. Brun, F. Carminati, F. Bruyant and M. Maire, *CERN Computer Newsletter* **200** (1990) 13.
[15] J.-M. Laget, Nucl. Phys. **A579** (1994) 333.
[16] J.-M. Laget, in *New Vistas in Electronuclear Physics*, Edts. E.L. Tomusiak, H.S. Caplan and E.T. Dressler (Plenum Press, New York, 1986) 361.
[17] R. Schiavilla *et al.*, Nucl. Phys. **A449** (1986) 219.

Bin	p_m	$d^5\sigma_{Exp.}$	$\Delta d^5\sigma_{Stat.}$	$\Delta d^5\sigma_{Syst.}$
	(MeV/c)	$\times 10^{-6}$ (fm^2/MeV/sr^2)		
1	25−40	2.10	±0.24	±0.17
2	40−55	1.55	±0.17	±0.13
3	55−70	1.16	±0.13	±0.10

TABLE I. Experimental differential cross sections.

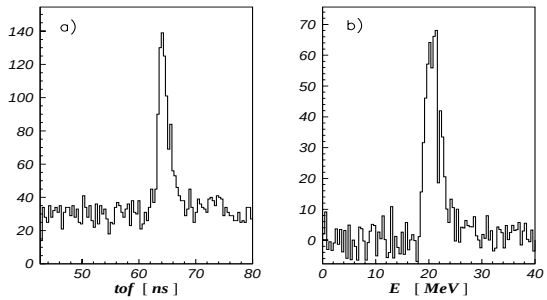

FIG. 1. a) ToF spectrum for neutrons in E_1 after all corrections discussed in the text, and b) missing-energy spectrum for the reaction ^{4}He(e,e′n)^{3}He after background subtraction.

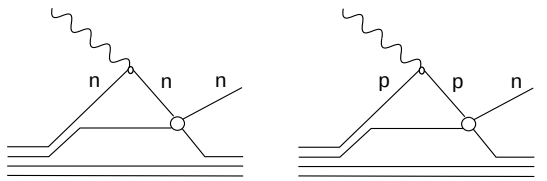

FIG. 2. The dominant FSI graph is broken down into elastic neutron rescattering (left) and charge-exchange proton rescattering (right).

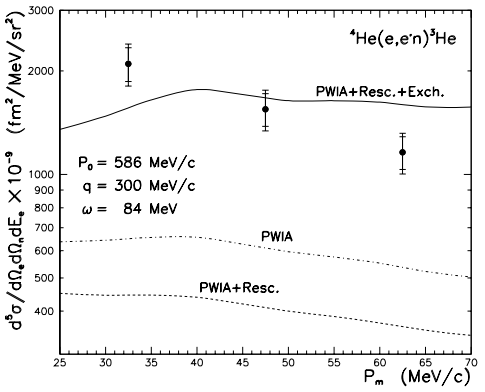

FIG. 3. The experimental cross section (dots) for the reaction ^{4}He(e,e′n)^{3}He compared to microscopic calculations [15].